REINFORCED CONCRETE WALL-FRAME STRUCTURES SUBJECTED TO DYNAMIC AND STATIC LOADINGS -- Model tests and the simulations ---

Kenji Koike[I], Yutaro Omote[I], Hiroaki Eto[I], Toshikazu Takeda[II]

SUMMARY

The paper presents test results of four identical reinforced concrete wall-frame structures under dynamic and static loadings. Each test specimen was a one-tenth (1/10) of full scale in size, three-bay, seven-storied plane shear wall-frame structure. A mathematical model was developed with considering inelasticity of each member in an attempt to correlate the experimental resutls. Good correlation of overall behavior was achieved when an appropriate hysteresis and damping were used.

I INTRODUCTION

One of the effective use of shear walls in seismic design of multi-storied structures is to make the shear walls and the boundary beams yield in bending instead of shear type of failure. Generally speaking, however, such structures are statically indeterminate in its failure mechanism and the internal force on walls or columns cannot be obtained by a limit analysis concept. According to the background above stated, it may be necessary to establish a valid inelastic analysis method for better understanding of ductile wall-frame structures and the design criteria should be examined by some tools such as experimental work and its exact simulation.

II STATIC AND DYNAMIC TESTS OF WALL-FRAME STRUCTURES

2.1 Design procedure of a specimen

A design procedure of a specimen in this paper was as follows.

i) Assumed an external loading distribution as inverse-triangular shape along the height.

ii) Calculated the yield moment of girders and then found the total reaction forces at the bottom. Absolute values of horizontal load along the height was decided by an equilibrium of overturning moment at the bottom.

iii) Each story shear force was then calculated and the shear force on exterior columns were derived, redistributing end moment of beams in proportion to the stiffness of columns above and below the node in consideration.

iv) Shear force on wall was calculated by subtracting the column shear from story shear force.

v) Reinforcing bar arrangement on the bottom story of wall was so designed as to fail in bending. The presumption of the failure mode was based on a Dr. Hirosawa's proposed formula[1] as:

if $Q_m/{}_cQ_{wu1} \leqq 0.75$ then flexural failure
if $0.75 \leqq Q_m/{}_cQ_{wu1} \leqq 1.25$ then flexural or shear failure
if $1.25 \leqq Q_m/{}_cQ_{wu1}$ then shear failure

where Q_m : ultimate flexural strength by Dr. Umemura's e-function
${}_cQ_{wu1}$: ultimate shear strength by an equation of

$${}_cQ_{wu1}=\{0.0679P_t{}^{0.23}(F_c+180)/\sqrt{M/QD+0.12}+2.7\sqrt{\sigma_{wh}P_{wh}}+0.1\sigma_0\}\cdot b_e\cdot j$$

The terms in the equation of P_t in percent is a tension bar ratio, F_c

I Researcher, Technical Research Institute of OHBAYASHI-GUMI LTD.
II Supervising Researcher, same above

is a compressive strength of concrete, σ_{wh} is yielding stress of shear reinforcement, P_{wh} is shear reinforcement ratio of wall, σ_o is an average compressive stress for gross sectional area, M/QD is a shear span ratio, b_e is an equivalent width of wall, d is a distance from the compressive fiber of concrete to the center of tension side column and j is 7/8d. The unit of stress and length are kg/cm^2 and cm, respectively.

vi) Girders and exterior columns were so designed as to fail in bending.

2.2 Construction of specimen

Four identical specimens of three-bay, seven-storied wall-frame structures were made as shown in Fig. 2.1. Three of them were provided for dynamic tests on a shaking table and the other one was for statically horizontal loading test. The characterization of each specimen is shown in Table 2.1. The scaling of overall structure and the consisted members are approximately one-tenth (1/10) of actual size. The dimensions and the rebar arrangements are shown in the figure. The material properties are listed in Table 2.2 where the mortar strengthes are varied for each test specimen because the time tested is different.

Additional steel weights were mounted at every beam-column joints in order to simulate the actual floor load of a building. Weight of mass at a joint was 264 kgs at interior and 143 kgs at exterior column joint which became totally of 5698 kgs. The axial compressive stress at the bottom of column was 51.3 kg/cm^2 and 27.8 kg/cm^2 for interior and exterior columns, respectively.

2.3 Test program

2.3.1 Shaking table tests

Three specimens were tested on a shaking table at Ohbayashi-gumi Ltd., whose exciting capacity was ten Ton-G. Mechanism of roller supports in horizontal direction were provided at the third and sixth story level so as to prevent out-of-plane deformation of the structure. As shown in Table 2.1, diversity of three specimens were their input wave forms. Input ground motion for specimen D1 was Tokachi-oki earthquake (1968) Hachinohe harbour NS component record with a duration time of about forty seconds, that was an actual time scale. The test was repeated two times (RUN-1,2), changing the input acceleration levels. Specimen D2 was excited by "enveloped-sin" wave specially made and its predominant frequency was matched at every stage of the expected first mode frequency of the structure. The test was repeated four times (RUN-1,2,3,4), changing the input level, so that progressing inelastic behavior was observed. The third specimen D3 was for Miyagi earthquake (June, 1978) TOHOKU Univ. NS component record. Actual duration time of the record, about thirty seconds, was contracted by the time scale of one-half (1/2) for test program in considering its spectrum tendency. The first run (RUN-1) made enough the specimen beyond yielding by the order of ductility factor 1.7. Although the test was continued to the second run (RUN-2), too much input acceleration made the weighted mass impact a guide roller.

2.3.2 Statical loading test

Figure 2.2 represents the test set-up of horizontally cyclic loading system. Loading points were distributed along the height at the seventh, sixth, fifth and third story level located on the shear wall. Vertically pin-jointed arms of A and B in the figure were provided both back and fore surface of the structure and then concentrated at point C. Cyclic load was applied at point D by using PC-steels and center hole jacks.

The distribution of loading ratio along the height was decided in order to simulate the shear and overturning moment distribution of the specimen to that of calculated values by applying the first mode shape of dynamic loads as shown in Fig. 2.3. So the ratio became as 1.0 : 1.0 : 0.57 : 1.09 for the seventh, sixth, fifth and third story, respectively. The horizontal loading sequence was followed by a part of response results of test D1 (dynamic test) at the seventh story displacement as shown in Fig. 2.4. Steel masses were also mounted for vertical load.

2.4 Dynamic test results

Figure 2.5 shows the final stage of each structure. Trend of progressive damages were the same for all specimens. A part of maximum response values for every specimens are listed in Table 2.3. An example of time history vibrating mode shape of displacement along the height is shown in Fig. 2.6 in case of test D1, RUN-1.

2.5 Static test results

The final failure is shown in Fig. 2.5. Shear cracks were extended up to the third story which was same as dynamic tests. The relation between total shear force and top displacement is shown in Fig. 2.7. Even after the rotation angle of 30/1000, strength degradation was not apparent and at the stage of 95/1000, 74% of the maximum load was still sustained.

Displacement mode shape along the height under some positive cycle loadings are plotted as shown in Fig. 2.8. Within a range of small loading level, the mode shape was similar to that of the calculated elastic first mode of vibration and characterized as combined bending and shear type of mode. An inverse-triangular mode shape was observed at the final stage where the structure formed an ultimate failure mechanism.

III MATHEMATICAL MODEL OF A WALL-FRAME STRUCTURE

3.1 Introductory remarks

Simulation analyses of static and dynamic tests were conducted by using a computer program developed for exact calculation of inelastic behavior of reinforced concrete structures. The formulation of equations and the other informations are described precisely in a paper of this conference by a part of same authors.[2]. A mathematical model of tested frame and the hysteretic behavior of every member element are only discussed in this chapter.

3.2 Inealasticity of elements

Four tested specimens, same in dimension, are substituted into a two-bay and seven-storied plane frame as shown in Fig. 3.1. The deformation considered are bending, shear and axial for column and wall elements, bending and shear for girders but shear deformation at beam-column joints are neglected in this analysis because the joint are considered to be rigid.

The wall elements, actually an equivalent column elements, and column elements are divided into thirteen horizontally sliced sub-elements in each story height. Every sub-elements have an individual non-linear moment-curvature relationship. Cyclic hysteresis rule was assumed as shown in Fig. 3.1. Elastic-inelastic behavior for shear deformation (γ) against average shear stress (τ) was also considered for each wall. Degradation of shear rigidity after shear cracks occured was assumed as one-tenth (1/10) of elastic rigidity. Cyclic behavior for shear force is same as bend-

ing moment hysteresis rule only in the range before yielding. A validity of these assumption were verified by analysis of the isolated three storied wall previously tested.[4]

Inelastic spring mechanism was assumed at an end of boundary beam to wall. Individual test program of beam-wall element was conducted and correlation between the test results and the assumed hysteresis rule are shown in Fig. 3.1.

Rotation due to the slippage of the tensile reinforcement of the beam from the joint of column was also taken into account. The rotation angle at the yielding of tension steel is a function of average bond stress (τ_a) and herein assumed to be $0.5\sqrt{F_c}$(MPA) by referring to a paper by Galvin[5].

With consideration of the slippage behavior, cyclic hysteresis rule was assumed as shown in Fig. 3.1. Individual test program of beam-column element was conducted and the results was correlated with the assumptions as shown in the figure.

IV SIMULATED TEST RESULTS

4.1 Simulation results for static test

Simulation analysis was conducted first for the static reversal loading test in order to verify the validity of the mathematical model discussed in Chapter-3. Hysteretic behavior of every element was already examined by the individual test program as stated in 3.2. Loading cycles for calculation were selected as Nos.-8, 12 and final cycles associated with the experimental loading program as shown in Fig. 2.4. A relationship between total load and the top displacement are plotted in Fig. 4.1, where rigid line represents the test results and dotted line is the calculated value.

Figure 4.2 shows the results by limit analysis method. The maximum load of the test was 2.61 tons while the calculated ultimate load was 2.24 tons which was 14% lower than the test results.

4.2 Simulation results for dynamic tests

The calculated maximum response values are shown in Table 2.3 comparing with the test results. For specimen D1, because the time duration of the tested responses were too much long for computation, the time between 6.0 and 10.0 seconds from the initial were taken into account for RUN-1 and almost similar for RUN-2. This was not an exact simulation of the test but almost covered the static loading program. For specimen D2, four test runs were calculated continuously with each duration time of two seconds. Only RUN-1 was calculated for specimen D3 by a reason stated in 2.3.1.

Figure 4.3 shows the examples of response wave forms for test D1 and D2 comparing the measured with calculated. Figure 4.4 shows an example of calculated base shear vs. top displacement in case of test D1. Figure 4.5 shows an example of calculated vibrating mode shape in case of test D1 comparing with the corresponding displacement of statical simulation results stated in 4.1. Figure 4.6 shows an example of progressing crack of concrete and yielding of re-bars in case of test D1 by calculation.

Spectrum simulation was conducted for calculated response in case of specimen D3, RUN-1. A transfer function of top story to the base, for

example, are shown in Fig. 4.7 compared with that of test results.

4.3 Discussion

Both the static and dynamic test results were simulated by a mathematical model discussed in Chapter-3. Statical simulation coincided fairly well with the test results which confirmed the evaluation of elastic and inelastic stiffness, hysteretic assumptions of member elements and base fixed condition of the physical model. Dynamic simulations demonstrated that if the statical simulation could be achieved well and if the adequate dampings were assumed, then the prediction of the dynamic response might be well attained by similar mathematical model.

Since the study presented herein is limited to plane structure of laboratory test specimens, a possibility of predicting the elastic-inelastic response of reinforced concrete wall-frame structure might be suggested.

V CONCLUSIONS

i) As expected in design of a specimen, yielding of every end of girders and bottom ends of both columns and shear wall at the first story were achieved under static and dynamic loadings and final compression failure was observed at the bottom of inner columns after very large deflection.

ii) The calculated acceleration and displacement at each floor which took into account the restoring force characteristics of every member element were reasonablly comparable with those measured.

iii) In accordance with the external force level increased by static or dynamic loadings, the predominant displacement mode shape of a structure changed from the elastic first mode of vibration into an inverse-triangular shape which was a mode of ultimate mechanism. This may suggest an adequency of using inverse-triangular shape of force distribution along the height in the process of ultimate state design of shear wall-frame structure.

iv) The shear wall had a large ductility when it was designed by a philosophy described in this paper, however, the compression failure of columns adjacent to the wall observed in these tests suggested a necessity of establishing more detailed criteria for design of ductile shear wall.

References:

(1) Hirosawa, M., "Past Experimental Results on Reinforced Concrete Shear Walls and Analysis on them" (in Japanese) Kenchiku Kenkyu Shiryo, No.6, March 1975, Building Research Institute, Ministry of Construction

(2) Eto, H., and Takeda, T., "Dynamic Collapse Tests of Reinforced Concrete Frame Structures with a Column Subjected to High Compressive Stress" Pre-prints of 7-WCEE, September 1980.

(3) Takeda, T., Sozen, M. A. and Nielsen, N.N., "Reinforced Concrete Response to Simulated Earthquakes" Journal of the Structural Division, ASCE, Vol.96, No.ST12, December 1970.

(4) Koike, K., Imoto, K. and Takeda, T. "Investigation of R/C Frame-Wall Structures (Part 1) - Tests of Bending Failure Type Shear Walls -" (in Japanese) Report of the Technical Research Institute, Ohbayashi-Gumi, Ltd. No.18, February 1979.

(5) Gavlin, N. L., "Bond Characteristics of Model Reinforcement" Civil Engineering Studies, Structural Research Series, No.427, University of Illinois, Urbana, 1976.

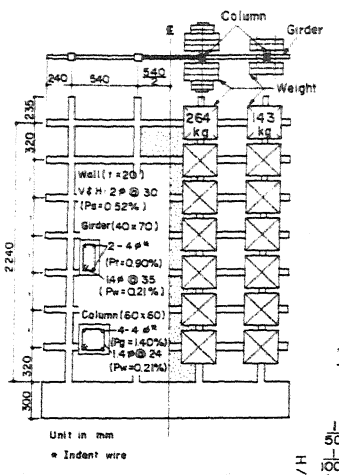

Fig. 2. 1 Specimen

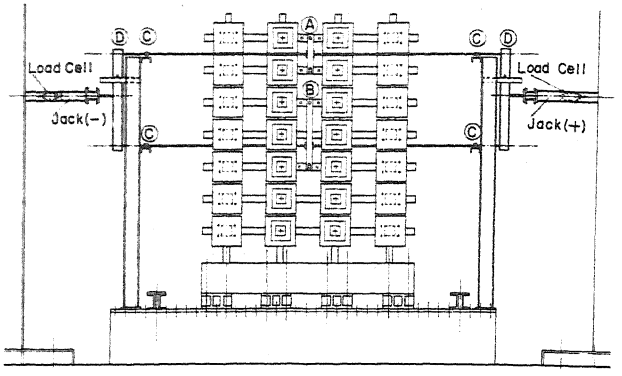

Fig. 2. 2 Loading System

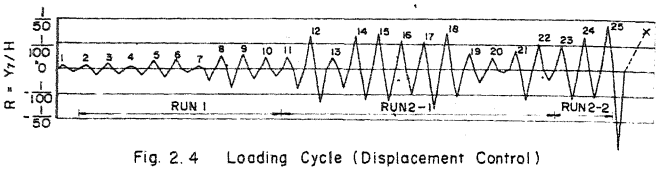

Fig. 2. 4 Loading Cycle (Displacement Control)

Table 2. 1 Test Identifications

Mark	Loading	Input Wave
S	static	Cyclic horizontal (25 cycles)
D1	dynamic	Tokachi-oki (RUN-1, 2)
D2	dynamic	Enveloped-sin (RUN-1, 2, 3, 4)
D3	dynamic	Miyagi-ken oki (RUN-1, (2))

Table 2. 2 Material Properties (unit in kgf/cm^2)

	wire	member	σy	σmax	Es(x10^6)
Steel	4φ indent wire	beam, column	2810	3670	1.99
	2φ wire	wall	2950	3850	—
	4φ wire	hoop	3250	4480	—

	specimen	Ec(x10^5)	σc	εc(x10^6)
Mortar	S	1.88	242	1930
	D1	1.57	202	2490
	D2, D3	2.02	254	2430

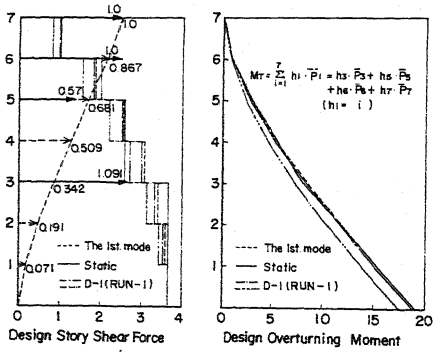

Fig. 2. 3 Horizontal Force Distribution

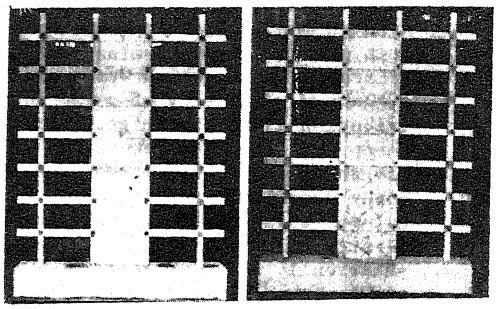

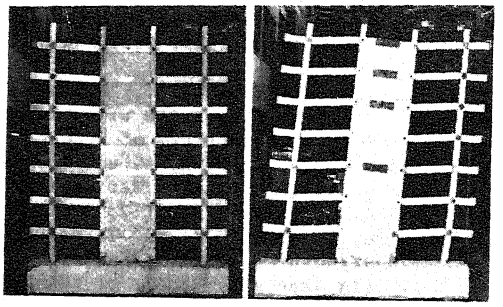

Fig. 2. 5 Photos of Final Failure

Table 2.3 List of Maximum Values

	Test	D1			D2			D3		
	Story	M	C	M/C	M	C	M/C	M	C	M/C
	Input Acc.	Max.411, Min.−638			Max.540, Min.−640			Max.460, Min−521		
Acc. (gal)	7 Max.	999	878	1.08	1103	1070	0.98	917	756	1.21
	Min.	−952	−935		−1017	−1084		−1004	−829	
	5 Max.	806	686	1.23	708	616	1.18	682	590	1.19
	Min.	−739	−566		− 754	− 625		− 735	−605	
	3 Max.	621	670	0.96	839	513	1.51	577	495	1.07
	Min.	−572	− 574		− 813	− 580		− 610	−618	
	1 Max.	504	428	1.14	890	558	1.67	514	449	1.07
	Min.	−614	− 557		− 829	− 471		− 552	−543	
Disp. (m)	7 Max.	35.5	32.2	1.26	45.6	42.8	1.03	23.4	19.6	0.93
	Min.	−32.0	− 21.4		− 37.0	− 37.3		− 18.0	−24.7	
	5 Max.	29.0	23.2	1.34	28.7	30.5	0.91	19.2	14.3	1.04
	Min.	−23.0	− 15.6		− 23.4	− 26.7		− 14.5	−18.0	
	3 Max.	17.7	13.8	1.32	20.8	17.6	1.09	9.9	8.6	0.86
	Min.	−12.9	− 9.4		− 15.3	− 15.5		− 6.7	−10.8	
	1 Max.	6.8	4.1	1.55	8.5	4.9	1.44	3.8	2.6	0.98
	Min.	− 3.9	− 2.8		− 4.9	− 4.4		− 2.0	− 3.3	
$R=Y_r/H$ ($1\,0^{-3}$)		15.8	14.4	1.26	20.4	19.1	1.03	10.4	8.8	0.93
		− 14.3	− 9.6		− 16.5	− 16.7		− 8.0	−11.0	

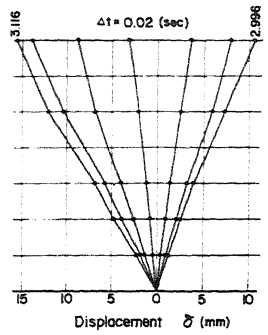

Fig. 2.6 Mode (DI)

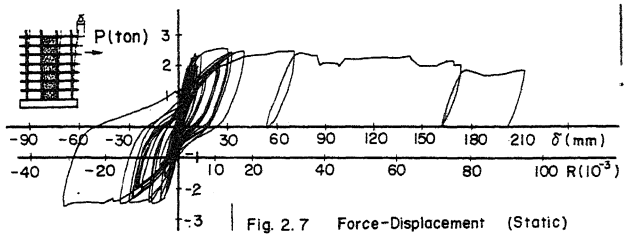

Fig. 2.7 Force-Displacement (Static)

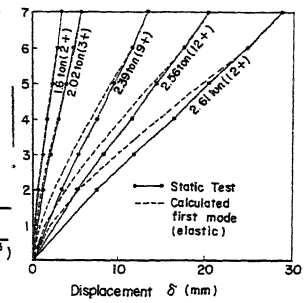

Fig. 2.8 Mode (S)

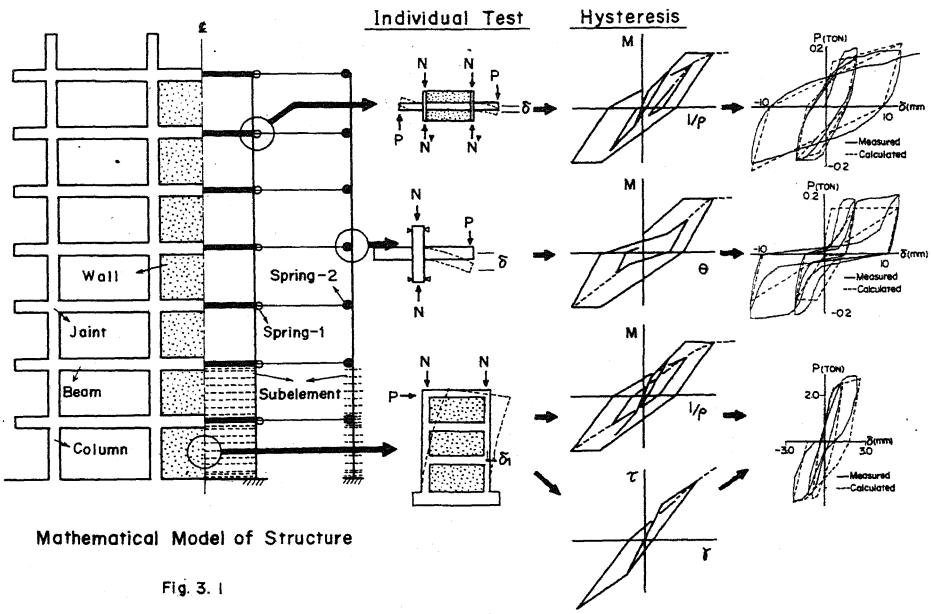

Mathematical Model of Structure

Fig. 3.1

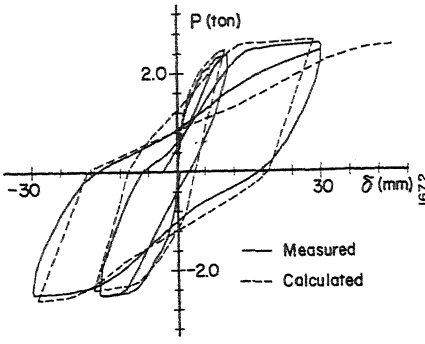

Fig. 4. 1 Static Simulation

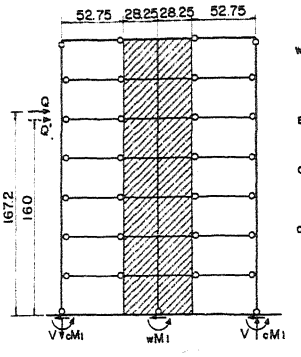

$wM_1 = 0.8 \cdot a_t \cdot \sigma_y \cdot D + 0.2 \cdot a_{sv} \cdot D + 0.5 \cdot N \cdot D \left(1 - N / b \cdot D \cdot F_c\right)$
$= 218\ t \cdot cm$

$sM = 0.9 \cdot a_t \cdot \sigma_y \cdot d$
$= 3.82\ t \cdot cm$

$cM_1 = 0.8 \cdot a_t \cdot \sigma_y \cdot D + 0.5 \cdot N \cdot D \left(1 - N / b \cdot D \cdot F_c\right)$
$= 8.71\ t \cdot cm$

$cM_7 = 3.81\ t \cdot cm$

$Q = (wM_1 + 2 \cdot cM_1 + 162 \cdot V) / 167.2$
$= 2.24\ t$

$Q' = (wM_1 + 2 \cdot cM_1 + 162 \cdot V) / 160$
$= 2.34\ t$

Fig. 4. 2 Ultimate Load

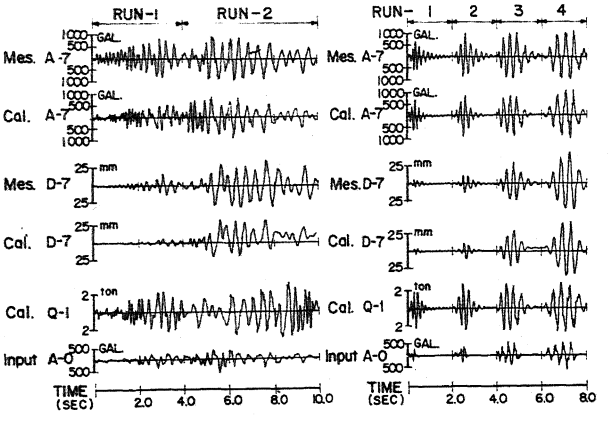

Fig. 4. 3 Dynamic Simulations

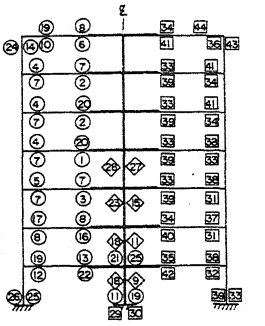

Fig. 4. 6 Failure Mechanism

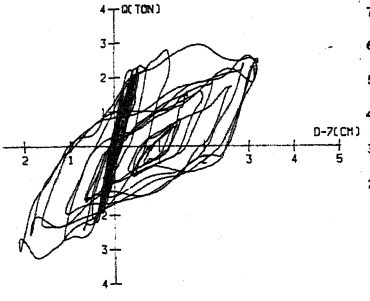

Fig. 4. 4 Calculated Shear-Disp. (D1)

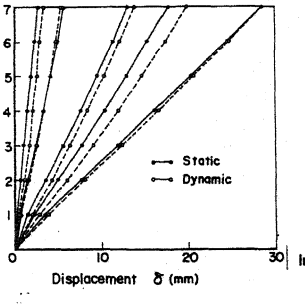

Fig. 4. 5 Mode (Calculated)

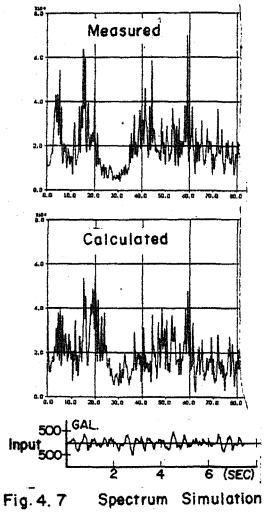

Fig. 4. 7 Spectrum Simulation